Contents lists available at ScienceDirect

Heliyon

journal homepage: www.cell.com/heliyon

Research article

Disconnection of the right superior parietal lobule from the precuneus is associated with memory impairment in oldest-old Alzheimer's disease patients

Pukovisa Prawiroharjo [a,d], Ken-ichiro Yamashita [a], Koji Yamashita [b], Osamu Togao [b], Akio Hiwatashi [c], Ryo Yamasaki [a], Jun-ichi Kira [a,*]

[a] Department of Neurology, Neurological Institute, Graduate School of Medical Sciences, Kyushu University, 3-1-1 Maidashi, Higashi-ku, Fukuoka 812-8582, Japan
[b] Department of Clinical Radiology, Graduate School of Medical Sciences, Kyushu University, 3-1-1 Maidashi, Higashi-ku, Fukuoka 812-8582, Japan
[c] Department of Molecular Imaging & Diagnosis, Graduate School of Medical Sciences, Kyushu University, 3-1-1 Maidashi, Higashi-ku, Fukuoka 812-8582, Japan
[d] Department of Neurology, Faculty of Medicine, Universitas Indonesia, Dr. Cipto Mangunkusumo National Central General Hospital, Jakarta, Indonesia

ARTICLE INFO

Keywords:
Alzheimer's disease
Default mode network
Dementia
Memory
Middle-old
Oldest-old
Neuroscience
Pathology
Neurology
Medical imaging
Radiology

ABSTRACT

There is a wide range of onset age in Alzheimer's disease (AD). Emerging evidence indicates variation of AD manifestations in oldest-old AD (OOAD); however, the pattern of cognitive dysfunctions remains unclear. We aimed to reveal cognitive performance characteristics and changes in brain functional connectivity in OOAD patients by a resting-state fMRI (rs-fMRI) study. We enrolled AD patients who had been referred to Kyushu University Hospital (KUH) or Sanno Hospital, and classified them into middle-old AD (MOAD) (65–79 years old) and OOAD (≥80 years old) according to the age of onset. Our subjects consisted of 19 OOAD, 17 MOAD, and 8 normal subjects. Cognitive performance was evaluated using Mini Mental State Examination-Japanese (MMSE-J) and Clinical Dementia Rating (CDR). rs-fMRI scanning and independent component analysis (ICA) were performed on Sanno Hospital patients and MOAD vs. OOAD patients were compared. The resulting significant regions were used as seeds for ROI-to-ROI analysis of the KUH dataset. Collectively, MMSE-J delayed recall subscores were significantly lower in OOAD patients compared with MOAD patients. ICA of the Sanno Hospital data indicated significant connectivity decrease in the default mode network (DMN) in the OOAD group compared with the MOAD group in the right superior parietal lobule (SPL). ROI-to-ROI analysis of the KUH dataset indicated significant disconnection in the OOAD group of the right SPL from the precuneus ($p < 0.01$). The functional connectivity from the right SPL to the precuneus was positively correlated with the MMSE-J delayed recall sub-score ($p = 0.03$) and negatively correlated with the CDR memory sub-scale ($p = 0.04$). These findings indicate that disconnection between the right SPL and the precuneus may contribute to worse memory capability in OOAD compared with MOAD.

1. Introduction

Global life expectancy has steadily and significantly increased from 67.2 years in 2010 to 70.8 years in 2015 (United Nations Department of Economic and Social Affairs, 2017). Japan has the highest life expectancy of any country at 83.7 years (World Health Organization, 2017), and a rapidly aging population (Arai et al., 2012), of which 26.6% are aged 65 or above (Statistics Bureau - Japan Ministry of Internal Affairs and Communication, 2016). The size of this aged population is projected to increase further (United Nations Department of Economic and Social Affairs, 2017) and together with this achievement comes an escalation in the prevalence of various kinds of degenerative disease.

Dementia impairs various cognitive abilities and reduces the capability to perform daily activities. The most common form of dementia is Alzheimer's disease (AD), which mostly affects people aged over 65 (Alzheimer's Association, 2017). A Japanese cohort assessed from 2002 to 2012 had double the AD incidence compared with a 1988–1998 cohort (14.6–28.2 per 1,000 person-years), mainly because of the aging population (Ohara et al., 2017). Compared with the rest of the world, Japan had the fifth largest dementia population in 2001 (Ferri et al., 2005) and rose to fourth place in 2015 (Prince et al., 2015).

* Corresponding author.
E-mail address: kira@neuro.med.kyushu-u.ac.jp (J.-i. Kira).

https://doi.org/10.1016/j.heliyon.2020.e04516
Received 8 July 2019; Received in revised form 26 January 2020; Accepted 16 July 2020

Despite its prevalence in people aged 65 or older, there are many studies reporting variants of AD in people younger than 65, known as early-onset Alzheimer's disease (EOAD). It has different clinical characteristics, i.e. memory sparing in the early stage, worse visuospatial and executive functions, attention and language, and faster disease progression compared with the more common late-onset Alzheimer's disease (LOAD), which mainly features memory impairment and has slower progression (Panegyres and Chen, 2013; Smits et al., 2012; van der Flier et al., 2011). The prevalence of EOAD is 5.5% of all AD cases (Zhu et al., 2015) and is mainly driven by mutations in amyloid precursor protein (*APP*), presenilin 1 (*PSEN1*), and presenilin 2 (*PSEN2*) genes, while mutations in the apolipoprotein ε4 (*APOEε4*) gene are prevalent in LOAD (Bertram and Tanzi, 2008; Panegyres and Chen, 2013). Anatomically, younger onset AD tends to have parietal-dominant pathology, with involvement of bilateral parietal, precuneus, and bilateral dorsolateral frontal areas, but with sparing of medial temporal areas (Cho et al., 2013; Noh et al., 2014). Functional imaging found that EOAD has rapid progression of hypometabolism in parietal, frontal, basal ganglia, and thalamic areas (Kim et al., 2005), with disconnection in all networks, especially auditory-, sensory-motor, and dorsal-visual systems, and in the default mode network (DMN) (Adriaanse et al., 2014), while disconnection in LOAD begins in the DMN and spreads to internetworks with disease progression (Badhwar et al., 2017; Brier et al., 2014). Histologically, AD with younger onset shows higher neurofibrillary tangle density in cortical areas, but a lower density in the hippocampus compared with LOAD (Murray et al., 2011).

People in advanced old-age, which is currently the world's fastest growing population (Hudson and Goodwin, 2013), have an increased risk of physical and mental dysfunctions (Cohen-Mansfield et al., 2013). This population was first described as “oldest-old” by Kannisto and he suggested to define the term with a cut-off at 80 years of age (Kannisto, 1994), which has found consensus (Baltes and Smith, 2003, 1999; Haroutunian et al., 2008; Hudson and Goodwin, 2013; Katsumata et al., 2012; Lucca et al., 2015; Ritchie and Kildea, 1995).

A voxel-based morphometry study found loss of parieto-temporal and posterior cingulate gray matter in EOAD but not LOAD (Ishii et al., 2005). This suggests that there may be different variants of AD morphometric and histologic features in different age groups, which may be correlated with different pathology. Therefore, there may also be different alterations in brain functional connectivity between the oldest-old AD and younger AD patients. However, we could not find any studies directly comparing oldest-old and middle-old AD using the modern techniques of morphometry and functional imaging.

This study aimed to find differences between middle-old AD (MOAD) and oldest-old AD (OOAD) using the age of 80 as a cut-off. We assessed cognitive-behavior performance and brain functional connectivity and analyzed correlation between these parameters. Additionally, we focused our analysis on the DMN because it is closely involved in AD pathology (Greicius et al., 2004; Mevel et al., 2011); the DMN is a key network that deteriorates in EOAD and especially in LOAD (Badhwar et al., 2017; Brier et al., 2014).

2. Materials and methods

2.1. Ethical consideration

This study was approved by Kyushu University Institutional Review Board for Clinical Research and all procedures performed were in accordance with the ethical standards of the responsible committee on human experimentation (institutional and national) and with the Helsinki Declaration of 1975. Informed consent was obtained from all patients included in the study.

2.2. Subjects

We enrolled clinically diagnosed LOAD patients [≥ 65 years old (y.o.)] who were referred to Kyushu University Hospital (KUH) or Sanno Hospital, Japan, between 2012 and 2015 and classified them into age groups: MOAD (65–79 y.o., 19 subjects, mean age ±SD, 75.4 ± 4.6 y.o.; KUH:Sanno = 8:11), and OOAD (80 y.o. and older, 21 subjects, mean age ±SD, 84.8 ± 2.9 y.o.; KUH:Sanno = 14:7). AD diagnosis was made by two neurologists using National Institute on Aging and Alzheimer's Association criteria (McKhann et al., 2011). For comparison, we also enrolled thirteen age-matched normal subjects (mean age ±SD, 75.6 ± 5.6 y.o.).

2.3. Neuropsychiatric tests

Cognitive performance was evaluated using Mini Mental State Examination-Japanese (MMSE-J) (Folstein et al., 1975; Sugishita and Hemmi, 2010). We also used Clinical Dementia Rating (CDR) (Hughes et al., 1982), although this was only available at KUH. We used total MMSE-J scores and sub-scores for each domain, and total CDR scales and sub-scales for each domain for further analysis.

2.4. Image acquisition

Each subject underwent MRI scanning using a 3-Tesla scanner (Achieva TX, Philips Medical Systems). We first performed an initial scan to center the field of view on the subject's brain. We then performed a 3D T1-weighted turbo field echo scan for anatomical reference (repetition time [TR] = 8.1 ms; echo time [TE] = 3.8 ms; field of view (FOV) = 240 mm; matrix size = 40 × 240; slice thickness = 1.0 mm). Lastly, we performed a gradient-echo echo-planar sequence for functional imaging (TR = 2800 ms; TE = 30 ms; flip angle = 90°; 40 × 3 mm slices; in-plane resolution of 3 × 3 mm). Overall scanning lasted 7 min.

2.5. Imaging analysis

fMRI data were preprocessed using CONN toolbox version 17.f (https://www.nitrc.org/projects/conn) in SPM version 12 (http://www.fil.ion.ucl.ac.uk/spm/). The first five scans were excluded to achieve steady state conditions. Functional images underwent a standard pipeline of preprocessing steps. including realignment and unwarping, slice-timing correction, normalization, outlier detection, and finally spatial smoothing (full width at half maximum = 10 mm), which resulted in functional images in Montreal Neurological Institute (MNI)-space using an echo planar imaging (EPI) template (Calhoun et al., 2017). Separately, T1 structural images also underwent a standard pipeline of preprocessing steps, including direct structural segmentation and normalization.

To reduce motion-related effects during resting-state fMRI scanning, we set the functional outlier detection setting of the subject's motion threshold to 0.5 mm. Therefore, if the subject moved more than 0.5 mm in any of six dimensions the scan would be counted as an outlier because of head motion artifacts being detected by Conn quality assurance and artifact rejection software (www.nitrc.org/projects/artifact_detect/) (Whitfield-Gabrieli and Nieto-Castanon, 2012). We removed subjects who had an extreme number of outliers, defined as more than + 2SD of the respective hospital group, and matched the number of outliers between groups in each hospital (Kaiser et al., 2016) using the Mann-Whitney test, and between groups using the Kruskal-Wallis test. We then performed de-noising, which consisted of removing white matter and cerebrospinal fluid noise (each with five dimensions), scrubbing, motion regression, band-pass filtering (0.01–0.10 Hz), and linear detrending.

We used independent component analysis (ICA) to find the seed for ROI-to-ROI analysis. However, using the same data for seed selection and then analysis will result in unacceptably distorted, non-independent statistical tests (Kriegeskorte et al., 2009). Therefore, we performed ICA on the Sanno dataset to establish the seed because it had fewer AD subjects, and then performed ROI-to-ROI analysis using the KUH dataset. The preprocessed images were fed into the ICA pipeline of CONN toolbox version 17.f. We used a predefined MNI network atlas included with CONN. In first-level analysis, we used the ICA networks menu on the

CONN dashboard and performed group ICA analysis based on Calhoun's group-level ICA approach, which normalized data variance, concatenated BOLD signal data in the temporal dimension, estimated independent spatial components using fast ICA, and estimated individual subject-level spatial maps using back-projected group ICA data (Calhoun et al., 2001). We set the number of factors to 17 and the dimensionality reduction to 64. In second-level analysis, we made a subtraction map of the group contrast differences (normal > OOAD, normal > MOAD, and MOAD > OOAD) to identify age-related, disease-specific connectivity changes. Significant difference on ICA was assumed by a corrected p-value for cluster-level family-wise-error (p-FWE) of less than 0.05 (Calhoun and Adali, 2012). The same processes were also performed to compare middle-old (n = 8 from KUH and Sanno Hospital) and oldest-old (n = 5 from KUH and Sanno Hospital) normal subjects, to exclude the possibility that the aging process itself affects our conclusions.

Among brain networks, the DMN is well known to be affected in AD pathology; especially in AD-related memory impairment, and thus the network is often studied in AD patients (Brueggen et al., 2017; Greicius et al., 2004; Mevel et al., 2011; Rombouts et al., 2005); therefore we focused our analysis on the DMN.

The significantly different regions from the Sanno ICA were plotted as seeds for ROI-to-ROI analysis of the KUH dataset. The Pearson linear correlation coefficient between the time course of the signal in each ROI and the average signal of the seed was calculated using CONN. ROI-to-ROI one-sample T-Tests were used to elucidate significant connection between the seed and the ROI in each group, which was considered when the corrected p-value for cluster-level false-discovery-rate (p-FDR) was less than 0.05 (Bueno et al., 2018). In cases where the ROI-to-ROI analysis revealed significant connection between targets and seed, the ROI analysis included the targets, which were defined anatomically from the MNI template.

We then performed correlation analysis between the resulting z-transformed r-values of significant ROI-to-ROI analysis (when comparing OOAD and MOAD) and the significant total MMSE-J score and each domain sub-score, along with total CDR scale and each domain sub-scale from previous neuropsychiatric tests. A Mann-Whitney test was performed for that purpose.

2.6. Statistical analysis

The age of each group was matched between hospitals using the Mann-Whitney test. Further analyses of total MMSE-J scores and sub-scores for each domain were performed in respective hospitals. We also carried out further analyses of total CDR scales and sub-scales for each domain in KUH. Spearman rank analysis was performed to verify the correlation between z-transformed r-values of significant ROIs and all previous neuropsychiatric results, which consist of total MMSE-J scores and sub-scores for each domain, and total CDR scales and sub-scales for each domain. All analyses were performed using Statistical Package for Social Sciences (SPSS®) version 22.0. Data are presented as the mean ± SD. Statistical significance was defined as p-value less than 0.05. Effect size for the results was also calculated using Cohen's d (Cohen, 1988).

3. Results

3.1. Cognitive performance results

We enrolled 48 subjects (8 normal, 19 MOAD, and 21 OOAD). Four subjects were excluded because of outlier criteria, leaving 44 subjects (8 normal, 17 MOAD, and 19 OOAD), with 23 subjects from KUH and 21 from Sanno Hospital. Each group was age-matched between hospitals (mean age ±SD, KUH vs. Sanno, normal: 73.7 ± 5.7 vs. 76.8 ± 5.9 y.o., p = 0.55; MOAD: 74.0 ± 5.2 vs. 75.9 ± 4.2 y.o., p = 0.38; OOAD: 84.3 ± 3.3 vs. 85.9 ± 2.7 y.o., p = 0.22). Outliers were matched between groups in each hospital (p KUH = 0.51; p Sanno = 0.91; p total = 0.92) and between hospitals in each group (p normal = 0.07; p MOAD = 0.42; p OOAD = 0.12).

Collective demographic data are presented in Table 1. Between MOAD and OOAD groups, there was significant difference in MMSE-J delayed recall sub-scores (MOAD vs. OOAD, 1.4 ± 1.2 vs. 0.6 ± 0.8, p = 0.03) in spite of borderline similar total MMSE-J scores (21.4 ± 3.5 vs. 18.8 ± 4.3, p = 0.08). There was no significant difference between groups in either time or place orientation sub-scores in MMSE-J (time orientation: 3.2 ± 1.3 vs.2.4 ± 1.3, p = 0.10; place orientation: 3.5 ± 1.0 vs. 3.6 ± 1.1, p = 0.59) or in MMSE-J immediate recall sub-scores (2.8 ± 0.5 vs. 2.8 ± 0.5, p = 0.75) and other MMSE-J sub-scores.

Among the 21 subjects from Sanno (5 normal, 9 MOAD, and 7 OOAD), there was no difference between MOAD and OOAD groups in total MMSE-J scores (22.1 ± 3.1 vs. 18.6 ± 4.9, p = 0.11), immediate recall sub-scores (3.0 ± 0.0 vs. 2.9 ± 0.4, p = 0.26), and delayed recall sub-scores (1.2 ± 1.2 vs. 0.4 ± 0.8, p = 0.17).

Among the 23 subjects from KUH (3 normal, 8 MOAD, and 12 OOAD) there was a tendency of significant difference in MMSE-J delayed recall sub-scores between MOAD and OOAD (1.6 ± 1.2 vs. 0.7 ± 0.9, p = 0.06), which was affirmed by a difference in CDR memory sub-scales (MOAD vs. OOAD: 1.1 ± 0.6 vs. 1.8 ± 0.6, p = 0.03, d = 1.2). There was no significant difference in total MMSE-J scores (20.6 ± 4.0 vs. 18.9 ± 4.1, p = 0.54), immediate recall sub-scores (2.6 ± 0.7 vs. 2.8 ± 0.6, p = 0.66), or other MMSE-J sub-scores between the two groups. There was also no significant difference in total CDR scales (1.2 ± 0.5 vs. 1.4 ± 0.7, p = 0.41) or other CDR sub-scales. KUH CDR data are presented in Table 2.

Table 1. Demographic data.

	Normal	MOAD	OOAD
N	8	17	19
Sex (female:male)	7:1	11:6	13:6
Age	75.6 ± 5.6	75.0 ± 4.6	84.8 ± 3.1*
Total MMSE-J	28.3 ± 1.5	21.4 ± 3.5	18.8 ± 4.3
Time orientation	4.5 ± 0.8	3.2 ± 1.3	2.4 ± 1.3
Place orientation	5.0	3.5 ± 1.0	3.6 ± 1.1
Immediate recall	3.0	2.8 ± 0.5	2.8 ± 0.5
Calculation	4.5 ± 0.8	2.7 ± 1.5	2.1 ± 1.3
Delayed recall	2.4 ± 0.7	1.4 ± 1.2	0.6 ± 0.8*
Naming	2.0	1.9 ± 0.2	2.0 ± 0.2
Repeating	0.9 ± 0.4	0.8 ± 0.4	0.7 ± 0.5
Three orders	3.0	2.7 ± 0.5	2.6 ± 0.5
Reading	1.0	1.0	1.0
Writing	1.0	0.8 ± 0.4	0.6 ± 0.5
Copying	1.0	0.7 ± 0.5	0.6 ± 0.5

* Statistically significant difference between MOAD and OOAD ($p < 0.05$).

Table 2. CDR data of KUH AD subjects.

	MOAD	OOAD
N	8	12
Total	1.2 ± 0.5	1.4 ± 0.7
Memory	1.1 ± 0.6	1.8 ± 0.6*
Orientation	1.1 ± 0.6	1.5 ± 0.7
Decision	1.1 ± 0.6	1.1 ± 0.4
Social	0.9 ± 0.2	1.1 ± 0.7
Family	1.3 ± 0.8	1.4 ± 0.7
Personal Care	0.9 ± 0.6	1.0 ± 0.6

* Statistically significant difference between MOAD and OOAD ($p < 0.05$).

3.2. Imaging results

ICA in the normal Sanno Hospital group found significant DMN connectivity (p-FWE < 0.05) among the precuneus, medial frontal cortex, left angular gyrus, right cuneal, right inferior lateral occipital cortex (LOC), and left superior LOC. In the MOAD group, we found significant DMN connectivity among the precuneus, right frontal pole, cerebellum, and left and right anterior middle temporal gyrus (MTG). In the OOAD group, we found significant DMN connectivity among the precuneus, left and right superior LOC, right frontal pole, left and right anterior MTG, right superior frontal gyrus (SFG), cerebellum, subcallosal cortex, left SFG, and left angular gyrus (Table 3). Lastly, with MOAD > OOAD contrast we found a significant decrease in DMN connectivity in the OOAD group compared with the MOAD between the right superior parietal lobule (SPL) (26 -52 48) (p-FDR < 0.05) and brainstem (6 -46 -66) (p-FDR < 0.05) (Table 3, Figure 1). There were no significant differences between groups using normal > OOAD and normal > MOAD contrasts, and *vice versa*. To exclude the effect of age on the ICA results, we performed the same analysis on thirteen normal subjects, consisting of middle-old (n = 8 from KUH and Sanno Hospital) and oldest-old (n = 5 from KUH and Sanno Hospital) subjects. This analysis showed no significant differences in the results between middle-old and oldest-old normal subjects for any particular region in the DMN.

In the next step, we used the significant regions from the aforementioned ICA DMN MOAD > OOAD contrast in the Sanno dataset as seeds in ROI-to-ROI analysis of the KUH dataset. We did not perform ROI-to-ROI analysis on the normal KUH group because of its small sample size (three subjects). We found significant connectivity (p-FDR < 0.05) between the right SPL (as the seed) to the left inferior frontal gyrus (IFG) pars triangularis, left posterior part of the inferior temporal gyrus (PITG), and precuneus (as ROI targets) when analyzing with MOAD > OOAD contrast (Figure 2) and z-transformed r-value of right SPL-to-left IFG pars triangularis (MOAD vs. OOAD: 0.1 ± 0.1 vs. -0.2 ± 0.1, $p < 0.01$, $d = 3.0$), -to-left PITG (0.0 ± 0.2 vs. -0.2 ± 0.1, $p < 0.01$, $d = 1.3$), and -to-precuneus (0.3 ± 0.2 vs. 0.0 ± 0.2, $p < 0.01$, $d = 1.5$) (Figure 3). ROI-to-ROI analysis with the brainstem as seed yielded no significant result.

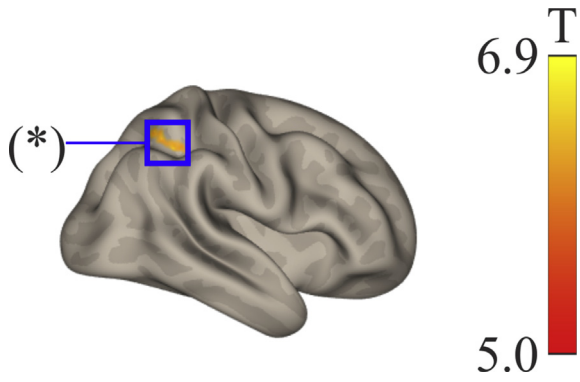

Figure 1. Independent component analysis (ICA) of the default mode network (DMN) of the Sanno Hospital dataset shows a significant regional difference for the MOAD minus OOAD subtraction in the right superior parietal lobule (SPL), marked by an asterisk (*) in this right lateral view.

Table 3. Independent component analysis of the Sanno Hospital dataset.

Subtraction Contrast	Region	x	y	z	Voxel	T
Normal	Precuneus	-4	-72	46	190	2061.1
		18	-70	38	26	371.1
		-12	-60	20	22	4.4
		8	-46	6	20	3.8
	Medial frontal cortex	-4	56	-10	69	723.3
	Left angular gyrus	-44	-62	20	30	4.4
	Right cuneal	16	-66	20	15	183.0
	Right inferior LOC	56	-64	12	20	3.9
	Left superior LOC	-38	-70	32	18	3.7
MOAD	Precuneus	-6	-60	34	17,943	40.2
	Right frontal pole	2	56	-14	884	8.6
		24	32	44	298	7.9
	Cerebellum	6	-60	-46	491	8.6
		-14	-84	-40	133	7.4
	Left anterior MTG	-62	-6	-20	129	10.5
	Right anterior MTG	60	-2	-18	96	6.2
OOAD	Precuneus	0	-64	34	7,896	80.8
	Left superior LOC	-30	-74	30	1,207	21.6
	Right superior LOC	34	-66	34	969	14.6
	Right frontal pole	8	62	-4	701	37.9
	Left anterior MTG	-58	-2	-22	213	14.1
	Right SFG	26	32	40	203	12.6
	Right anterior MTG	58	-8	-28	178	13.1
	Cerebellum	6	-56	-42	88	13.1
		26	-48	-48	40	8.7
	Subcallosal cortex	10	24	-14	62	11.4
	Left SFG	-24	28	42	57	8.8
	Left Angular Gyrus	-36	-78	-42	51	9.3
MOAD > OOAD	SPL	26	-52	48	74	6.9
	Brainstem	6	-46	-66	93	5.0

LOC = lateral occipital cortex; MTG = middle temporal gyrus; SFG = superior frontal gyrus; SPL = superior parietal lobule.

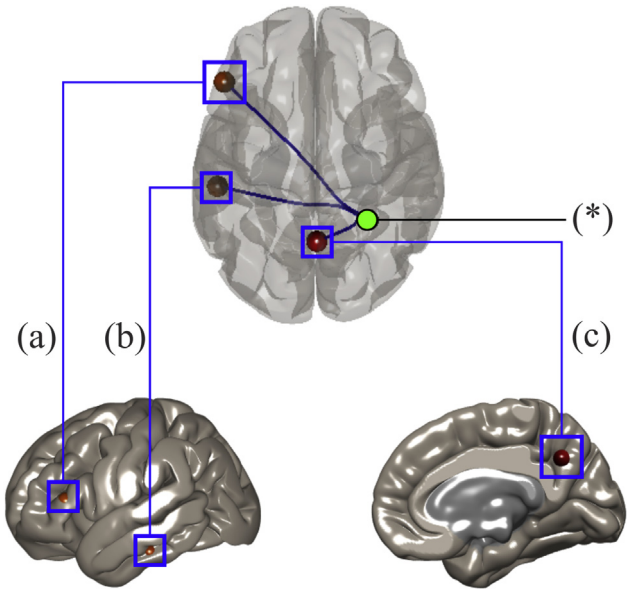

Figure 2. Significant regions of interest with the right superior parietal lobule as seed for the MOAD minus OOAD subtraction are marked by an asterisk (*). (a) Left inferior frontal gyrus pars triangularis, (b) the posterior part of the left inferior temporal gyrus (PITG) (on left lateral view), and (c) precuneus (on right medial view).

As a final step, we used Spearman's rank analysis and found that there were significant correlations between right SPL-to-precuneus connectivity and MMSE-J delayed recall sub-scores ($r = 0.49$, $p = 0.03$, $d = 1.1$), and significant anti-correlation between right SPL-to-precuneus connectivity and CDR memory sub-scales ($r = -0.46$, $p = 0.04$, $d = 1.0$) in AD groups (Figure 4). The connectivity from right SPL-to-left IFG pars triangularis and -to-left PITG had no significant correlation to either MMSE-J delayed recall sub-scores or CDR memory sub-scales.

4. Discussion

The neuropsychiatric tests in OOAD patients indicated more significant memory impairment compared with MOAD subjects, leading us to focus our analysis on the DMN. ICA of the Sanno Hospital groups found reduced DMN connectivity among the right temporal pole, right SPL, and brainstem in the OOAD group. However, when used as a seed in the KUH dataset, only the right SPL (part of the DMN) had significantly reduced connections to the left IFG pars triangularis, left PITG, and precuneus (part of the DMN). Correlation analysis showed that only the reduced connectivity between the right SPL and the precuneus was significantly correlated with reduced memory capability, which was reflected in the decreased MMSE-J delayed recall sub-scores and increased CDR memory sub-scales.

4.1. Role of the SPL and precuneus in memory processing

Previous studies have demonstrated the role of the right SPL in memory, especially for, but not limited to, spatial storage (Wager and Smith, 2003) and episodic memory (Wagner et al., 2005). The SPL may also be important in managing working memory, including updating, ordering, and manipulations (Crocco et al., 2018; Koenigs et al., 2009; Wager and Smith, 2003; Zou et al., 2013), and thus may be required for learning new information. Several studies also found that the SPL (Bakkour et al., 2013; Prvulovic et al., 2002; Teipel et al., 2007) and precuneus (Buckner et al., 2005; Klaassens et al., 2017; Scahill et al., 2002) were atrophied in AD. The precuneus also has a significant role in memory, especially for spatial and verbal storage (Wager and Smith, 2003) and episodic memory (Wagner et al., 2005). It is also associated

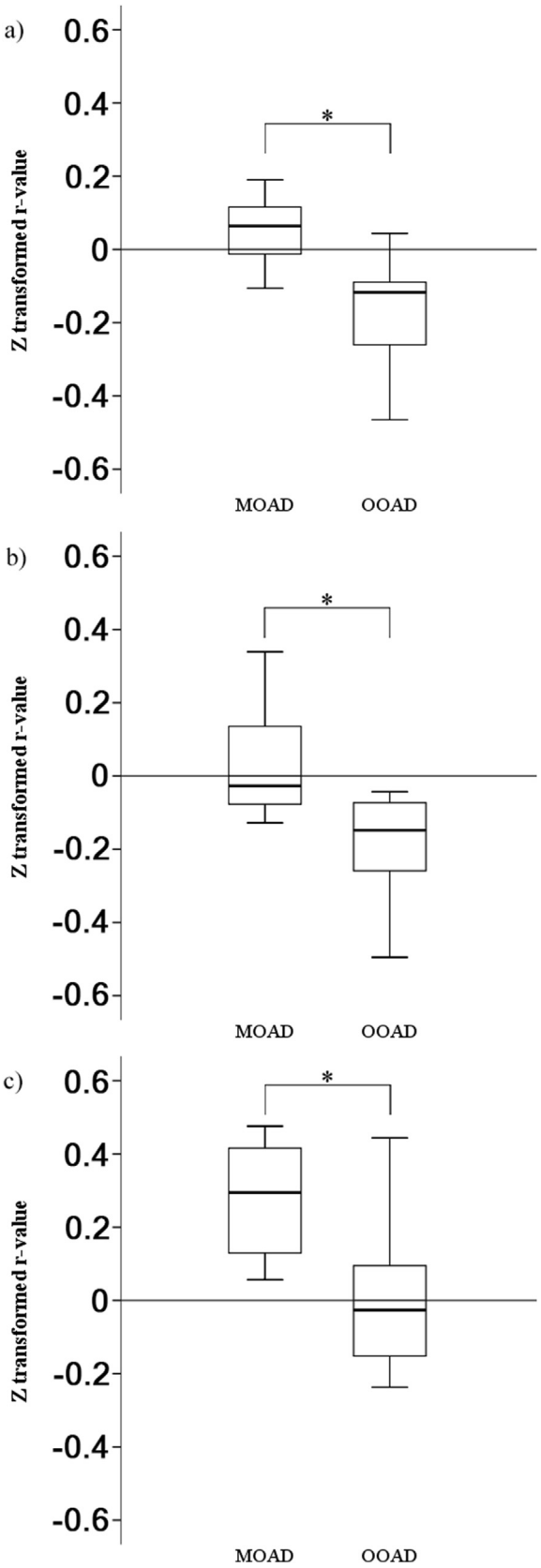

Figure 3. Boxplot of connectivity Z-transformed r-values from the right SPL to the (a) left IFG pars triangularis, (b) left PITG, and (c) precuneus in KUH patients. IFG = inferior frontal gyrus, PITG = posterior part of the inferior temporal gyrus. * Statistically significant connectivity differences ($p < 0.05$) between MOAD and OOAD.

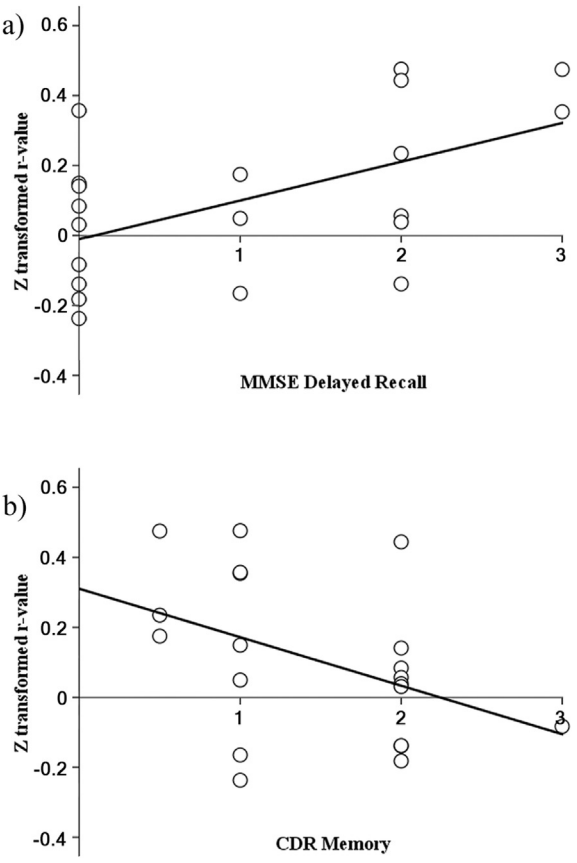

Figure 4. Scatterplot between right SPL-to-precuneus z-transformed r-values and (a) MMSE-J delayed recall sub-scores (r = 0.49, p = 0.03), and (b) CDR memory sub-scales (r = -0.46, p = 0.04) of KUH patients.

with learning (Crocco et al., 2018) and working memory performance (Zou et al., 2013). Meanwhile, the ITG is associated with object storage (Wager and Smith, 2003).

The right SPL and precuneus, and the connection between the two, are part of the DMN, a network of regions across the brain that has increased activities at rest but is suspended during goal-directed behaviors (Raichle, 2015; Raichle et al., 2001). Previous studies have established the importance of the DMN in memory and other cognitive functions (Greicius et al., 2004) while reduced DMN activity is observed in oldest-old subjects (Badhwar et al., 2017; Brier et al., 2014). This, in turn, might result in reduced memory capability, manifested as the difference in the MMSE-J delayed recall sub-scores and CDR memory sub-scales between the MOAD and OOAD groups. Our results also showed that right SPL-to-precuneus connectivity significantly correlated with MMSE-J delayed recall sub-scores and CDR memory sub-scales, i.e., higher connectivity between these regions translated into better memory capability, marked by higher MMSE-J delayed recall sub-scores and lower CDR memory sub-scales.

4.2. Association between functional connectivity in OOAD and pathological protein

Meanwhile, the connectivities between right SPL-to-left IFG pars triangularis and -to-left PITG were significantly lower in OOAD compared with MOAD, indicating that these disconnections might be part of AD pathophysiology in the oldest-old group. This reflects widespread brain network disconnections (Brier et al., 2012) that spreads beyond the DMN as the disease progresses (Badhwar et al., 2017; Brier et al., 2014). In addition, no significant differences between middle-old and oldest-old normal subjects were seen indicating that the aging process itself could be ignored in DMN hypoconnectivity. However, their z-transformed r-values did not significantly correlate with either MMSE-J delayed recall sub-scores or CDR memory sub-scales, indicating that these disconnections might affect brain functions outside of cognitive and memory domains.

A recent study found that amyloid-beta-positive individuals showed hypoconnectivity in the intra- and extra-DMN because Tau-PET signals were elevated (Schultz et al., 2017), while the DMN is also often noted as a major deposition site for amyloid in AD (Buckner et al., 2009). Tauopathy is widely recognized in older AD (Dumurgier et al., 2017; Harrison et al., 2019); therefore, the hypoconnectivity of the SPL-to-precuneus (intra DMN) in our study, which also correlated with memory impairment, is consistent with these findings (Ward et al., 2015).

4.3. Limitation

The limitation of our study was the relatively small sample size, although the effect size of this study ranged from large to huge (Cohen, 1988). The lack of differences between middle-old and oldest-old normal subjects supports our hypothesis of pathological changes causing the observed changes in memory capability and brain connectivity; however, considering the limited number of normal subjects, chronological changes cannot be completely ruled out. We also only used simple memory function evaluations (MMSE-J and CDR) to find differences in all cognitive fields instead of focusing on memory. Further studies, especially those with emphasis on detailed memory function and diagnosis with a larger sample size, are warranted. Additionally, we were not able to obtain amyloid and tau biomarkers for PET to determine protein deposition to support our findings. We also did not perform brain volumetric analysis in this study. Despite these limitations, our study showed that there may be a difference in AD between middle-old and oldest-old patients, both in memory capability and brain connectivity. This should be taken into account in future studies, and for early detection and management of AD patients especially in oldest-old patients.

5. Conclusion

Disconnection between the right SPL and precuneus may contribute to worse memory capability in OOAD compared with MOAD. Further studies regarding these findings are warranted.

Declarations

Author contribution statement

Pukovisa Prawiroharjo, Ken-ichiro Yamashita, Jun-ichi Kira: Conceived and designed the experiments; Performed the experiments; Analyzed and interpreted the data; Wrote the paper.

Koji Yamashita, Osamu Togao, Akio Hiwatashi, Ryo Yamasaki: Performed the experiments; Wrote the paper.

Funding statement

This work was supported by Takeda Science Foundation for the Fiscal Year 2017 scholarship, LPDP for the Beasiswa Untuk Dosen Indonesia Luar Negeri 2018–2021 scholarship, and the Indonesian Ministry of Research, Technology and Higher Education.

Competing interest statement

The authors declare no conflict of interest.

Additional information

No additional information is available for this paper.

References

Adriaanse, S.M., Binnewijzend, M.A.A., Ossenkoppele, R., Tijms, B.M., van der Flier, W.M., Koene, T., et al., 2014. Widespread disruption of functional brain organization in early-onset Alzheimer's disease. PloS One 9, e102995.

Alzheimer's Association, 2017. 2017 Alzheimer's disease facts and figures. Alzheimer's Dementia 13, 325–373.

Arai, H., Ouchi, Y., Yokode, M., Ito, H., Uematsu, H., Eto, F., et al., 2012. Toward the realization of a better aged society: messages from gerontology and geriatrics. Geriatr. Gerontol. Int. 12, 16–22.

Badhwar, A., Tam, A., Dansereau, C., Orban, P., Hoffstaedter, F., Bellec, P., 2017. Resting-state network dysfunction in Alzheimer's disease: a systematic review and meta-analysis. Alzheimer's Dement. Diagnosis Assess. Dis. Monit. 8, 73–85.

Bakkour, A., Morris, J.C., Wolk, D.A., Dickerson, B.C., 2013. The effects of aging and Alzheimer's disease on cerebral cortical anatomy: specificity and differential relationships with cognition. Neuroimage 76, 332–344.

Baltes, P.B., Smith, J., 2003. New frontiers in the future of aging: from successful aging of the young old to the dilemmas of the fourth age. Gerontology 49, 123–135.

Baltes, P.B., Smith, J., 1999. Multilevel and systematic analyses of old age: theoretical and empirical evidence for a fourth age. Handbook of Theories of Aging, p. 816.

Bertram, L., Tanzi, R.E., 2008. Thirty years of Alzheimer's disease genetics: the implications of systematic meta-analyses. Nat. Rev. Neurosci. 9, 768–778.

Brier, M.R., Thomas, J.B., Ances, B.M., 2014. Network dysfunction in Alzheimer's disease: refining the disconnection hypothesis. Brain Connect. 4, 299–311.

Brier, M.R., Thomas, J.B., Snyder, A.Z., Benzinger, T.L., Zhang, D., Raichle, M.E., et al., 2012. Loss of intranetwork and internetwork resting state functional connections with Alzheimer's disease progression. J. Neurosci. 32, 8890–8899.

Brueggen, K., Fiala, C., Berger, C., Ochmann, S., Babiloni, C., Teipel, S.J., 2017. Early changes in alpha band power and DMN BOLD activity in Alzheimer's disease: a simultaneous resting state EEG-fMRI study. Front. Aging Neurosci. 9.

Buckner, R.L., Sepulcre, J., Talukdar, T., Krienen, F.M., Liu, H., Hedden, T., et al., 2009. Cortical hubs revealed by intrinsic functional connectivity: mapping, assessment of stability, and relation to Alzheimer's disease. J. Neurosci. 29, 1860–1873.

Buckner, R.L., Snyder, A.Z., Shannon, B.J., LaRossa, G., Sachs, R., Fotenos, A.F., et al., 2005. Molecular, structural, and functional characterization of Alzheimer's disease: evidence for a relationship between default activity, amyloid, and memory. J. Neurosci. 25, 7709–7717.

Bueno, A.P.A., Pinaya, W.H.L., Moura, L.M., Bertoux, M., Radakovic, R., Kiernan, M.C., et al., 2018. Structural and functional papez circuit integrity in amyotrophic lateral sclerosis. Brain Imaging Behav.

Calhoun, V.D., Adali, T., 2012. Multisubject independent component analysis of fMRI: a decade of intrinsic networks, default mode, and neurodiagnostic discovery. IEEE Rev. Biomed. Eng. 5, 60–73.

Calhoun, V.D., Adali, T., Pearlson, G.D., Pekar, J.J., 2001. A method for making group inferences from functional MRI data using independent component analysis. Hum. Brain Mapp. 14, 140–151.

Calhoun, V.D., Wager, T.D., Krishnan, A., Rosch, K.S., Seymour, K.E., Nebel, M.B., et al., 2017. The impact of T1 versus EPI spatial normalization templates for fMRI data analyses. Hum. Brain Mapp. 38, 5331–5342.

Cho, H., Jeon, S., Kang, S.J., Lee, J.-M., Lee, J.-H., Kim, G.H., et al., 2013. Longitudinal changes of cortical thickness in early- versus late-onset Alzheimer's disease. Neurobiol. Aging 34, 1921 e9-1921.e15.

Cohen-Mansfield, J., Shmotkin, D., Blumstein, Z., Shorek, A., Eyal, N., Hazan, H., 2013. The old, old-old, and the oldest old: continuation or distinct categories? An examination of the relationship between age and changes in health, function, and wellbeing. Int. J. Aging Hum. Dev. 77, 37–57.

Cohen, J., 1988. Statistical Power Analysis for the Behavioral Sciences, second ed. Lawrence Earlbaum Associates, Hillsdale.

Crocco, E.A., Loewenstein, D.A., Curiel, R.E., Alperin, N., Czaja, S.J., Harvey, P.D., et al., 2018. A novel cognitive assessment paradigm to detect Pre-mild cognitive impairment (PreMCI) and the relationship to biological markers of Alzheimer's disease. J. Psychiatr. Res. 96, 33–38.

Dumurgier, J., Hanseeuw, B.J., Hatling, F.B., Judge, K.A., Schultz, A.P., Chhatwal, J.P., et al., 2017. Alzheimer's disease biomarkers and future decline in cognitive normal older adults. J. Alzheim. Dis. 60, 1451–1459.

Ferri, C.P., Prince, M., Brayne, C., Brodaty, H., Fratiglioni, L., Ganguli, M., et al., 2005. Global prevalence of dementia: a Delphi consensus study. Lancet 366, 2112–2117.

Folstein, M.F., Folstein, S.E., McHugh, P.R., 1975. "Mini-mental state". A practical method for grading the cognitive state of patients for the clinician. J. Psychiatr. Res. 12, 189–198.

Greicius, M.D., Srivastava, G., Reiss, A.L., Menon, V., 2004. Default-mode network activity distinguishes Alzheimer's disease from healthy aging: evidence from functional MRI. Proc. Natl. Acad. Sci. 101, 4637–4642.

Haroutunian, V., Schnaider-Beeri, M., Schmeidler, J., Wysocki, M., Purohit, D.P., Perl, D.P., et al., 2008. Role of the neuropathology of Alzheimer disease in dementia in the oldest-old. Arch. Neurol. 65, 1211–1217.

Harrison, T.M., La Joie, R., Maass, A., Baker, S.L., Swinnerton, K., Fenton, L., et al., 2019. Longitudinal tau accumulation and atrophy in aging and alzheimer disease. Ann. Neurol. 85, 229–240.

Hudson, R.B., Goodwin, J., 2013. The global impact of aging: the oldest old. Public Policy Aging Rep. 23, 2–25.

Hughes, C.P., Berg, L., Danziger, W.L., Coben, L.A., Martin, R.L., 1982. A new clinical scale for the staging of dementia. Br. J. Psychiatry 140, 566–572.

Ishii, K., Kawachi, T., Sasaki, H., Kono, A.K., Fukuda, T., Kojima, Y., et al., 2005. Voxel-based morphometric comparison between early- and late-onset mild Alzheimer's disease and assessment of diagnostic performance of z score images. AJNR. Am. J. Neuroradiol. 26, 333–340.

Kaiser, R.H., Whitfield-Gabrieli, S., Dillon, D.G., Goer, F., Beltzer, M., Minkel, J., et al., 2016. Dynamic resting-state functional connectivity in major depression. Neuropsychopharmacology 41, 1822–1830.

Kannisto, V., 1994. Development of Oldest-Old Mortality, 1950-1990: Evidence from 28 Developed Countries. Odense University Press, Odense.

Katsumata, Y., Todoriki, H., Higashiuesato, Y., Yasura, S., Willcox, D.C., Ohya, Y., et al., 2012. Metabolic syndrome and cognitive decline among the oldest old in Okinawa: in search of a mechanism. The KOCOA Project. J. Gerontol. Ser. A Biol. Sci. Med. Sci. 67A, 126–134.

Kim, E.J., Cho, S.S., Jeong, Y., Park, K.C., Kang, S.J., Kang, E., et al., 2005. Glucose metabolism in early onset versus late onset Alzheimer's disease: an SPM analysis of 120 patients. Brain 128, 1790–1801.

Klaassens, B.L., van Gerven, J.M.A., van der Grond, J., de Vos, F., Möller, C., Rombouts, S.A.R.B., 2017. Diminished posterior precuneus connectivity with the default mode network differentiates normal aging from Alzheimer's disease. Front. Aging Neurosci. 9, 97.

Koenigs, M., Barbey, A.K., Postle, B.R., Grafman, J., 2009. Superior parietal cortex is critical for the manipulation of information in working memory. J. Neurosci. 29, 14980–14986.

Kriegeskorte, N., Simmons, W.K., Bellgowan, P.S.F., Baker, C.I., 2009. Circular analysis in systems neuroscience: the dangers of double dipping. Nat. Neurosci. 12, 535–540.

Lucca, U., Tettamanti, M., Logroscino, G., Tiraboschi, P., Landi, C., Sacco, L., et al., 2015. Prevalence of dementia in the oldest old: the Monzino 80-plus population based study. Alzheimer's Dementia 11, 258–270 e3.

McKhann, G.M., Knopman, D.S., Chertkow, H., Hyman, B.T., Jack, C.R., Kawas, C.H., et al., 2011. The diagnosis of dementia due to Alzheimer's disease: recommendations from the National Institute on Aging-Alzheimer's Association workgroups on diagnostic guidelines for Alzheimer's disease. Alzheimer's Dementia 7, 263–269.

Mevel, K., Chételat, G., Eustache, F., Desgranges, B., 2011. The default mode network in healthy aging and Alzheimer's disease. Int. J. Alzheimer's Dis. 2011, 1–9.

Murray, M.E., Graff-Radford, N.R., Ross, O.A., Petersen, R.C., Duara, R., Dickson, D.W., 2011. Neuropathologically defined subtypes of Alzheimer's disease with distinct clinical characteristics: a retrospective study. Lancet Neurol. 10, 785–796.

Noh, Y., Jeon, S., Lee, J.M., Seo, S.W., Kim, G.H., Cho, H., et al., 2014. Anatomical heterogeneity of Alzheimer disease: based on cortical thickness on MRIs. Neurology 83, 1936–1944.

Ohara, T., Hata, J., Yoshida, D., Mukai, N., Nagata, M., Iwaki, T., et al., 2017. Trends in dementia prevalence, incidence, and survival rate in a Japanese community. Neurology 88, 1925–1932.

Panegyres, P.K., Chen, H.-Y., 2013. Differences between early and late onset Alzheimer's disease. Am. J. Neurodegener. Dis. 2, 300–306.

Prince, M., Wimo, A., Guerchet, M., Gemma-Claire, A., Wu, Y.-T., Prina, M., 2015. World Alzheimer Report 2015: the global impact of dementia - an analysis of prevalence, incidence, cost and trends. Alzheimer's Dis. Int. 84.

Prvulovic, D., Hubl, D., Sack, A.T., Melillo, L., Maurer, K., Frolich, L., et al., 2002. Functional imaging of visuospatial processing in Alzheimer's disease. Neuroimage 17, 1403–1414.

Raichle, M.E., 2015. The brain's default mode network. Annu. Rev. Neurosci. 38, 433–447.

Raichle, M.E., MacLeod, A.M., Snyder, A.Z., Powers, W.J., Gusnard, D.A., Shulman, G.L., 2001. A default mode of brain function. Proc. Natl. Acad. Sci. 98, 676–682.

Ritchie, K., Kildea, D., 1995. Is senile dementia "age-related" or "ageing-related"?–evidence from meta-analysis of dementia prevalence in the oldest old. Lancet 346, 931–934.

Rombouts, S.A.R.B., Barkhof, F., Goekoop, R., Stam, C.J., Scheltens, P., 2005. Altered resting state networks in mild cognitive impairment and mild Alzheimer's disease: an fMRI study. Hum. Brain Mapp. 26, 231–239.

Scahill, R.I., Schott, J.M., Stevens, J.M., Rossor, M.N., Fox, N.C., 2002. Mapping the evolution of regional atrophy in Alzheimer's disease: unbiased analysis of fluid-registered serial MRI. Proc. Natl. Acad. Sci. 99, 4703–4707.

Schultz, A.P., Chhatwal, J.P., Hedden, T., Mormino, E.C., Hanseeuw, B.J., Sepulcre, J., et al., 2017. Phases of hyperconnectivity and hypoconnectivity in the default mode and salience networks track with amyloid and tau in clinically normal individuals. J. Neurosci. 37, 4323–4331.

Smits, L.L., Pijnenburg, Y.A.L., Koedam, E.L.G.E., van der Vlies, A.E., Reuling, I.E.W., Koene, T., et al., 2012. Early onset Alzheimer's disease is associated with a distinct neuropsychological profile. J. Alzheim. Dis. 30, 101–108.

Statistics Bureau - Japan Ministry of Internal Affairs and Communication, 2016. Population. Statistical Handbook of Japan 2016. Tokyo.

Sugishita, M., Hemmi, I., JADNI, 2010. Validity and reliability of the mini mental state examination-Japanese (MMSE-J): a preliminary report. Jpn J. Cogn. Neurosci. 12, 186–190.

Teipel, S.J., Born, C., Ewers, M., Bokde, A., Reiser, M., Möller, H., et al., 2007. Multivariate deformation-based analysis of brain atrophy to predict Alzheimer's disease in mild cognitive impairment. Neuroimage 38, 13–24.

United Nations Department of Economic and Social Affairs, 2017. World Population Prospects: the 2017 Revision. Population Division.

van der Flier, W.M., Pijnenburg, Y.A.L., Fox, N.C., Scheltens, P., 2011. Early-onset versus late-onset Alzheimer's disease: the case of the missing APOE ε4 allele. Lancet Neurol. 10, 280–288.

Wager, T.D., Smith, E.E., 2003. Neuroimaging studies of working memory: a meta-analysis. Cognit. Affect Behav. Neurosci. 3, 255–274.

Wagner, A.D., Shannon, B.J., Kahn, I., Buckner, R.L., 2005. Parietal lobe contributions to episodic memory retrieval. Trends Cognit. Sci. 9, 445–453.

Ward, A.M., Mormino, E.C., Huijbers, W., Schultz, A.P., Hedden, T., Sperling, R.A., 2015. Relationships between default-mode network connectivity, medial temporal lobe structure, and age-related memory deficits. Neurobiol. Aging 36, 265–272.
Whitfield-Gabrieli, S., Nieto-Castanon, A., 2012. Conn: a functional connectivity toolbox for correlated and anticorrelated brain networks. Brain Connect. 2, 125–141.
World Health Organization, 2017. World Health Statistics 2017 : Monitoring Health for the SDGs. World Health Organization.
Zhu, X.-C., Tan, L., Wang, H.-F., Jiang, T., Cao, L., Wang, C., et al., 2015. Rate of early onset Alzheimer's disease: a systematic review and meta-analysis. Ann. Transl. Med. 3, 38.
Zou, Q., Ross, T.J., Gu, H., Geng, X., Zuo, X.-N., Hong, L.E., et al., 2013. Intrinsic resting-state activity predicts working memory brain activation and behavioral performance. Hum. Brain Mapp. 34, 3204–3215.